Desalination and Water Treatment
www.deswater.com

doi: 10.1080/19443994.2015.1096214

57 (2016) 19402–19410
September

Simultaneous removal of nitrogen and phosphorus using autoclaved aerated concrete particles in biological aerated filters

Dong Chen[a], Chao Yu[a], Teng Bao[a,b], Chengzhu Zhu[a], Chengsong Qing[a], Tianhu Chen[a,*]

[a]*Laboratory for Nanomineralogy and Environmental Material, School of Resources and Environmental Engineering, Hefei University of Technology, Hefei, China, Tel./Fax: +86 055162903990; emails: cdxman@hfut.edu.cn (D. Chen), 974318781@qq.com (C. Yu), tengbao1222@sina.com (T. Bao), czzhu@163.com (C. Zhu), csqing@hfut.edu.cn (C. Qing), chentianhu168@vip.sina.com (T. Chen)*
[b]*Science and Engineering Faculty, School of Chemistry, Physics and Mechanical Engineering, Queensland University of Technology, Brisbane, Australia*

Received 21 January 2015; Accepted 11 September 2015

ABSTRACT

Autoclaved aerated concrete particles (AACPs) were developed as alternative for the biofilter carriers. To obtain high biomass concentration, the biogenic stimulating properties of the AACPs were investigated. Meanwhile, the feasibility of using these particles as biological aerated filter media was assessed. The experimental results showed that the removal efficiencies of chemical oxygen demand (COD_{Cr}) and total nitrogen (TN) both increased with the increase in the ratio of COD_{Cr} to NH_4^+-N (C/N) in the biofilters. It could be demonstrated that the well-developed porous structures of AACPs were conducive to many microbial communities, resulting in an improvement of the permeability of biofilm layers and the pollutant removal efficiencies. The adoption of AACPs in such an environment significantly improved phosphate removal from wastewater. Our findings suggested that AACPs can play significant roles as carriers in simultaneous nitrification and denitrification by biological wastewater treatment systems.

Keywords: Autoclaved aerated concrete particles; Biofilm; Simultaneous nitrification and denitrification; Phosphate removal

1. Introduction

Autoclaved aerated concrete (AAC) is currently considered as "green" or "environmentally friendly" building materials [1]. AAC was developed in Sweden in the 1920s in response to increasing demands on timber supplies, and it is a lightweight manufactured building stone that composed of all natural raw materials and applied in various commercial, industrial, and residential systems [1–3].

With the rapid development of AAC, autoclaved aerated concrete particles (AACPs) as common building wastes have drawn considerable attentions because of their large quantities and difficulty in disposal [4–6]. Numerous studies have been conducted to comprehensive utilization of AACPs, such as using AACPs as raw materials to produce cement (replacing clay) and other building materials [7–11].

*Corresponding author.

Recently, waste materials such as waste ceramics and polyethylene plastic have been successfully used as ceramites for biological aerated filter (BAF), which provides a new approach to dispose AACPs building wastes [12]. The ceramites are widely used as filter media in wastewater treatment plants in China [13–18]. However, the raw materials for ceramites mainly consist of farmland clay, which is a valuable agricultural resource. Loss of clay in large quantities may threaten the sustainable development of agriculture in China [15,19]. Therefore, identifying a promising substitute of farmland clay to produce filter media is crucial for the development of both wastewater treatment and agriculture. In the present study, AACPs building wastes were selected as alternative for clay due to their similar mineral contents.

Lightweight and porous AACPs were successfully prepared in the present study. The chemical speciation was also investigated. The microstructure of AACPs revealed the existence of many unevenly distributed pores (0.1–0.5 mm of pore size), which was suitable for the attachment of micro-organisms during the growth process. The present study aims to determine whether AACPs can be used as carriers for biofilters and exhibit biogenic stimulating properties necessary to obtain high biomass. The proposed advantages of AACPs, such as low cost and minimizing potential environmental impact were evaluated. With such significant advantages considered, one important objective of this study was to investigate how COD/NH_4^+-N(C/N) ratios affect pollutant removal performance and establish effective parameters for evaluation. Our specific research objectives are:

(1) To identify the contribution of AACPs on NH_4^+-N removal in start-up lab-scale biofilters.
(2) To analyze the mechanisms of chemical oxygen demand (COD_{Cr}), NH_4^+-N, total nitrogen (TN), Phosphate removal by biofilters at different C/N ratios.

2. Material and methods

2.1. Lab-scale biofilters

A lab-scale upflow BAF was set up as shown in Fig. 1. Lab-scale biofilter columns were made of acrylic. The columns had an upflow configuration with 1.50 m in height and 0.07 m in inner diameter. The influent wastewater was evenly filled into a network of distribution holes at the bottom of the biofilter system, and the treated effluent was collected through the collecting pipes at the top of the system. The wastewater and the AACPs in the lab-scale biofilter columns were constantly aerated by an air blower to improve oxygen transmission.

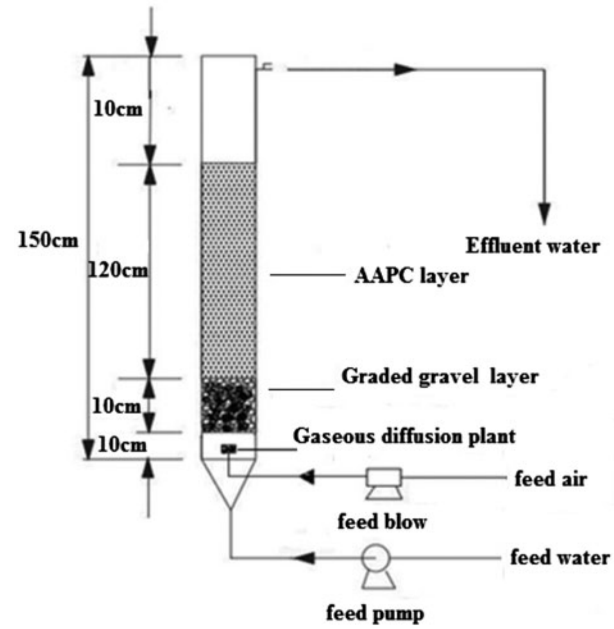

Fig. 1. Schematic diagram of the BAF system.

2.2. AACPs characterization

The multi-point BET surface area of the AACPs was measured using a Quantachrome nova 3000e automated surface area and pore size analyzer. Prior to the surface area measurements, the samples were degassed in vacuum at 300˚C for 6 h. The chemical composition of samples by X-ray fluorescence (XRF) was measured on a Shimadzu XRF-1800 with Rh radiation.

Parameters of AACPs were determined according to the Filter Material for Water Treatment (CJ/T 43-2005) standard including bulk and particle densities. As shown in Table 1, the compressive strength of the AACPs was analyzed by using an INSTRON KC-2A material testing machine (China).

2.3. Analyses of water quality

Water samples from inlet and outlet pipes were collected and stored at 0˚C for less than 24 h prior to evaluation of water quality. The COD concentrations were measured according to the standard potassium dichromate method and represented as COD_{Cr} [20]. Colorimetric method was used to analyze ammonia nitrogen (NH_4^+-N), TN, and phosphorus. Dissolved oxygen (DO) concentration was measured with a portable

Table 1
The regulatory levels of AACPs and corresponding Nation Standard

No.	Item	Index	AACPs
1	Grain diameter (d/mm)	0.5–9.0	5–9
2	Silt carrying capacity (C_s/%)	≤1	3.34
3	Void fraction (υ/%)	≥40	71.48
4	Specific surface area (S_w/cm^2 g)	≥0.5 × 10^4	8.1 × 10^5
5	Piled density (ρ_p/g/cm^3)	–	0.53
6	Apparent density (ρ_{ap}/g/cm^3)	–	1.71
7	Compression strength (N)	–	35–43
8	Porosity (%)		89.21

digital DO meter (JPB-607, Shanghai, China). All chemical reagents used were analytical grade and purchased from Hefei Chemical Reagent Corporation (China).

2.4. Start-up of biofiltration systems

Activated sludge was collected from a full-scale municipal wastewater treatment plant (Wang–Xiao Ying Wastewater Treatment Plant, Hefei, China). Sludge supernatant was used as microbial biomass inoculum for seeding the AACPs.

Initially, 80% of wastewater inside the system was withdrawn, and an equal volume of the fresh wastewater was added every 2 d. After 8 d, the treated water in the systems was replaced every day with fresh wastewater for bacterial growth. The biofilm on the AACPs grew well (light yellow attached-growth flocculent mass was observed on the AACPs) after 3 weeks, and the systems were shifted to a continuous operation. The sludge and wastewater in the tank were constantly aerated using an SP-780 Super Pump air blower (China) to improve oxygen transmission.

After the start-up of the biofiltration system, the treated biofilm was immediately observed using a scanning microscope system. The surface morphology of the selected AACPs was examined using the environmental SEM model Philips XL30 ESEM. The grown biofilm was determined as described in a previous study [21]. The pore characteristics of the AACPs were determined according to the sandstone pore structure method of image analysis [22]. The development of biofilm on the AACPs was observed using a BX41 biological microscope (Olympus, Japan).

2.5. Operating conditions

The biological aerated filter (BAF) test was divided into four stages (as shown in Table 2). The operating conditions of AACP BAFs for each stage were identical, i.e. DO > 4 mg/L, air/water in the range of 2:1–3:1.

2.6. Evaluation of AACPs characterization

The resultant AACPs met parameters in the Filter Material for Water Treatment (CJ/T 43-2005) standards, including particle diameter and density, as shown in Table 1. Pictures of AACPs were shown in Fig. 2.

3. Results and discussion

3.1. Chemical composition

The chemical composition of AACPs determined by XRF was as follows: 44.88 wt% SiO_2, 24.98 wt% CaO, 16.06 wt% Al_2O_3, 4.16 wt% Fe_2O_3, and small amounts of K_2O, SiO_3, TiO_2, MgO, Na_2O, Cr_2O_3, and MnO. This result indicated that SiO_2, CaO, and Al_2O_3 made up the main components of the AACPs

3.2. Porous structure

In order to obtain direct evidences on environmental micro-organisms in open porosity of AACPs, a special pore structure method of image analysis reported by the literature [15] was used to quantitatively identify the size and shape of pores in a thin section of AACPs. Fig. 3(a) shows the intergranular pore textures observed in thin gray sections. And the size of interconnected porosity ranged from about 0.25 to 0.5 mm, as shown in Fig. 3(a) and (b). Since most bacteria were 0.5 μm or smaller in diameter, the figure indicated that the AACPs had a large volume of internal porosity that can accommodate guest microbes. In addition, the surrounding micro-organisms can sustain bacterial growth in the open porosity (Part c). By contrast, some

Table 2
Operating conditions

Water quality indexes and operating conditions						
Sample	PH	T (℃)	HRT (h)	COD_{cr} IC ± SD	NH_3-N IC ± SD	PO_4^{3-} IC ± SD
Stage one (60d)	6.9	25–30	7–7.09	52.59 ± 2.25	10.63 ± 0.6	0.52 ± 0.02
Stage two (10d)	7.3	25–30	7–7.09	29.93 ± 0.64	10.02 ± 0.17	0.52 ± 0.02
Stage three (10d)	6.7	20–25	7–7.09	79.92 ± 0.77	9.92 ± 0.19	0.51 ± 0.02
Stage four (10d)	6.5	20–23	7–7.09	99.15 ± 0.62	9.96 ± 0.28	0.51 ± 0.01
	COD_{cr}		NH_3-N		PO_4^{3-}	
	EC ± SD	RR ± SD	EC ± SD	RR ± SD	EC ± SD	RR ± SD
Stage one (60d)	20.41 ± 7.37	61.34 ± 13.43	1.55 ± 1.21	85.08 ± 11.77	0.16 ± 0.04	69.48 ± 7.82
Stage two (10d)	8.54 ± 2.51	71.50 ± 8.24	1.32 ± 0.26	86.83 ± 2.44	0.06 ± 0.03	87.44 ± 6.24
Stage three (10d)	19.70 ± 2.07	75.33 ± 2.72	2.58 ± 0.39	73.88 ± 4.34	0.09 ± 0.02	81.54 ± 3.77
Stage four (10d)	17.11 ± 2.95	82.73 ± 3.06	2.67 ± 0.25	73.18 ± 2.93	0.1 ± 0.02	80.35 ± 2.84

Notes: The values are removal rates in %; $COD_{cr}/NH_3\text{-N}/PO_4^{3-}$ values are influent concentrations mg/L Standard deviation—SD; Removal rates—RR; Effluent concentrations—EC; Influent concentrations—IC.

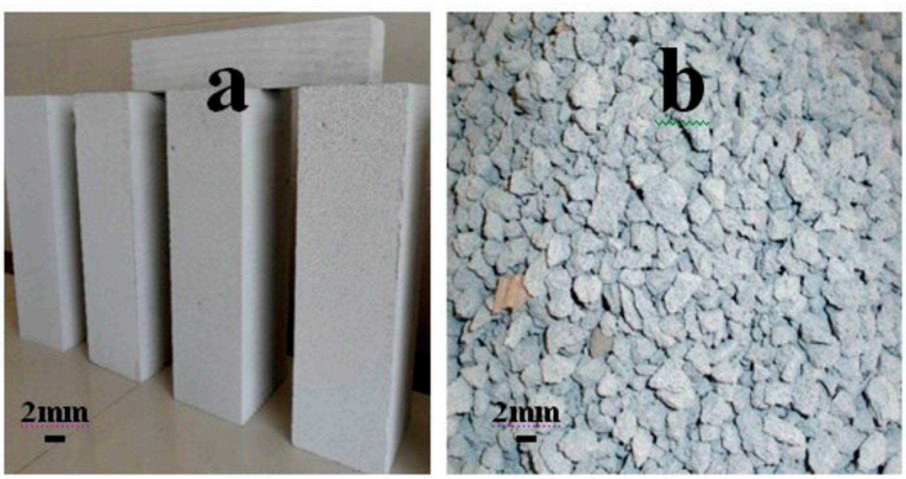

Fig. 2. Pictures of AACPs: (a) raw external surface of AACs and (b) raw external surface of AACPs.

closed pores in the AACPs (Part d) prevented the reproduction of microbes. Fig. 3(b) shows a narrow part interconnected by the throats. Gray sections vacuum impregnated with red-dyed epoxy (Part d) in the AACPs were observed from the fully interconnected pores with a diameter of 0.3 mm between the narrowest parts. The red-dyed epoxy in the porosity system must overcome the capillary resistance determined by the throat size of the interconnected pore before entering the porosity space, branching, and fairly isolating the almost connected throat narrow composition. This proved that these interconnected pores had a possibility for the entrance of microbes.

3.3. Performance of AACPs in BAF reactors at start-up

3.3.1. NH_4^+-N removal

The operating conditions of AACP BAFs in stage one were shown in Table 2. The influent and effluent NH_4^+-N in the AACP BAFs during the start-up stage was presented in Fig. 4. The AACP BAFs exhibited excellent NH_4^+-N removal efficiency and led to an increase in NH_4^+-N removal when the operation last for 60 d (Fig. 4). During the whole 60 d, the AACP BAFs exhibited excellent NH_4^+-N removal efficiency from 61.06 to 97.22%. When the operation reached 15 d, the concentrations of NH_4^+-N in the effluent

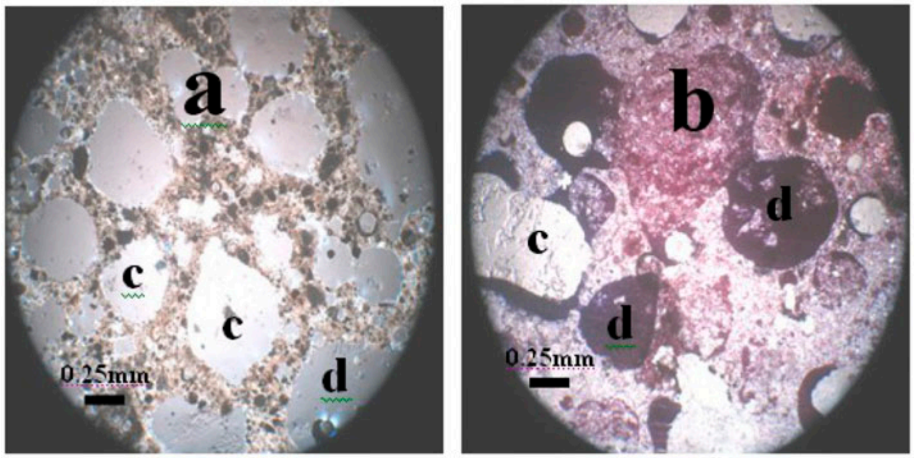

Fig. 3. The porosity of AACPs: (a) intergranular pores in AACPs and (b) internal surface in AACPs.

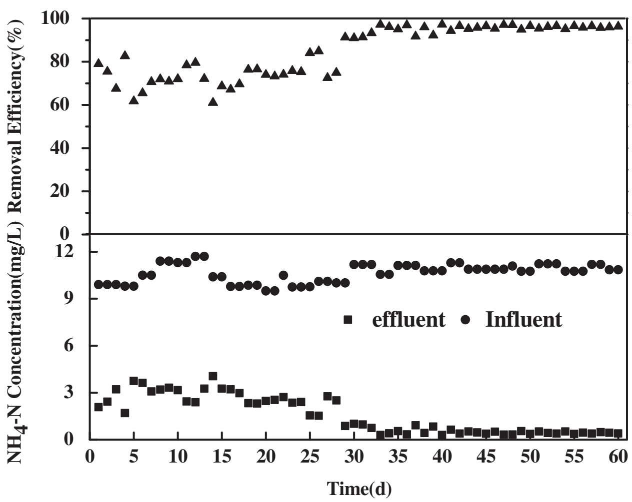

Fig. 4. Influent, effluent, and removal efficiency of NH_4^+-N.

varied from 2.3 to 4.0 mg/L, suggesting a decrease in NH_4^+-N removal efficiency (from 76.57 to 61.06%) and the reactor still required a longer duration for stabilization. During the subsequent 45 d, the concentrations of NH_4^+-N in the effluent of the AACP BAFs remained in the range of 0.3–1.55 mg/L.

The increase in the number of operating days resulted in mature biofilm development, favoring the growth of heterotrophic bacteria against autotrophic bacteria. In substrate enrichment, heterotrophic bacteria competed with autotrophic bacteria, and DO resulted in sharp increase in NH_4^+-N removal efficiency [23,24].

3.3.2. Morphological analyses (SEM)

The micrograph of the AACPs (Fig. 5(a)) clearly shows that some pores with diameters of 0.5–1.0 mm are regularly distributed on the surface. Fig. 5(b) shows that the microbes directly attached to the surface of the AACPs and the biofilm had been formed on the surface of the AACPs, as indicated by the connection of extracellular secretions [25]. The structures of the biofilm and the cells were maintained, with no indication of clogging or disintegration.

3.3.3. Microscopic observation of populations in biofilm

Optical microscopic observation (conducted at COD_{Cr}/NH_4^+-N ratio of 5) was illustrated in Fig. 6(a) and (b). It was found that there were micro-organisms in the biofilm, mainly including nitrifying bacteria. The presence of biofilm indicated satisfactory performance of biological wastewater treatment systems, and the stability of biofilm contributed to AACPs reduction. Accumulation of abundant micro-organisms on the AACPs surface and pores indicated efficient filling of organic matter and other substrates into the pore spaces, which can be attributed to the interconnected porous structures, i.e. the biogenic stimulating characteristics of AACPs, just as the literature [26] reported.

3.4. Performance of AACP BAFs under various operating conditions

The operating conditions of AACP BAFs for stage one to stage four are shown in Table 2). The AACP BAFs were operated at varying COD_{Cr}/NH_4^+-N (C/N) ratios (3, 5, 8, and 10). The concentration of NH_4^+-N of influent was maintained in the range of 9.5–11 mg/L. Meanwhile, the organic loading rates and the phosphate rates varied from 50 to 100 mg/L and 0.5 to 0.6 mg/L, respectively. Hydraulic retention time

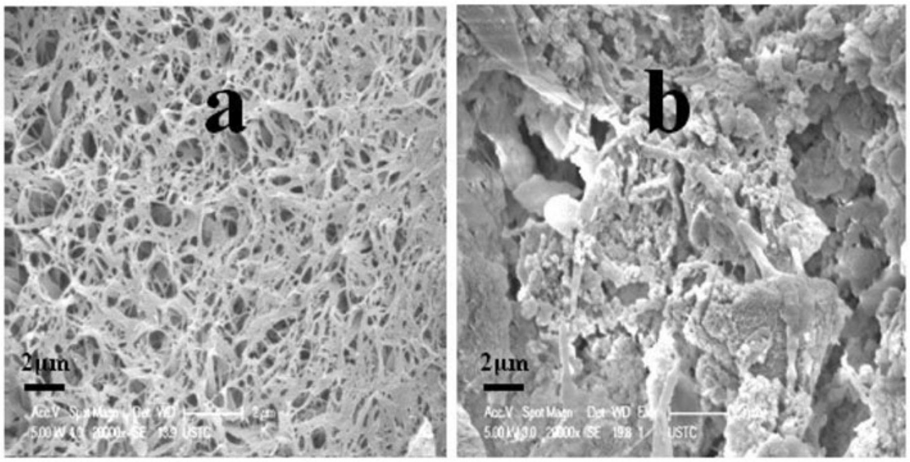

Fig. 5. SEM images of external surface in AACPs: (a) raw external surface of AACPs and (b) microbial load on external surface of AACPs.

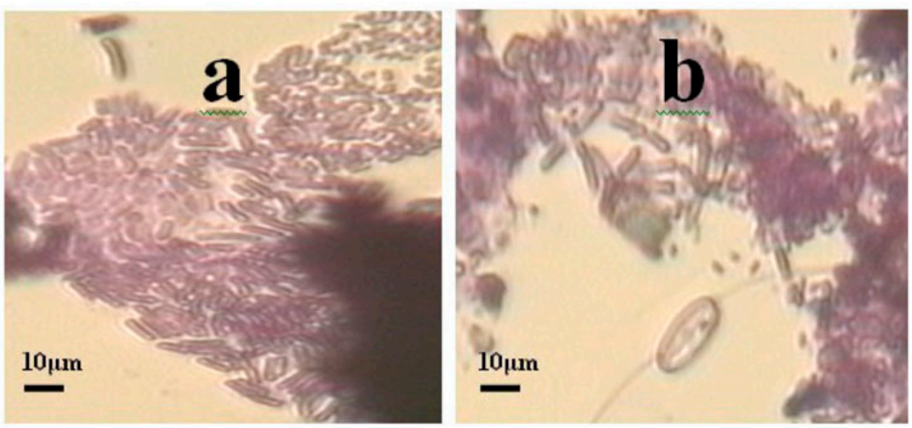

Fig. 6. The microscopic observation of biofilm in the systems.

(HRT) was 7.09 h. Fig. 8 shows the performances of the AACP BAFs indicated by the average removal of COD_{Cr}, NH_4^+-N, TN, and phosphate at different C/N ratios.

3.4.1. Effect of COD_{Cr}/NH_4^+-N on COD_{Cr} removal efficiencies

Fig. 7 shows the AACP BAFs ratios. COD_{Cr} removal varied from 60.21 to 84.56% at different C/N ratios. At C/N ratios of 3, 5, 8, and 10, the COD_{Cr} average removal rates were determined as 73.12, 72.65, 75.33, and 82.73%, respectively. However, the COD_{Cr} removal by the AACP BAFs sharply decreased with increasing C/N ratios. These observations confirmed that the C/N ratios significantly affect the removal efficiency of COD_{Cr}. With increased C/N ratios and a constant NH_4^+-N loading rate, the organic substrates were not completely degraded prior to discharge from the AACP BAFs.

As shown in the images of the biofilm and the corresponding analysis, the AACPs exhibited a uniform and well-developed pore structure. Such a structure allowed soluble organic matter and nutrient substances had access to deep holes, which optimized the application of AACPs. The increase in COD_{Cr}, i.e. C/N, in the system enhanced the rapid adsorption of soluble organics onto the organisms. This effect accelerated the first removal step of organic matter by transporting the organic matter from the wastewater to the biofilm. The available space for growth of micro-organisms, mass transfer rate of DO, and dispersion of biomass were also increased by extending soluble pollutants to the deep holes of AACPs.

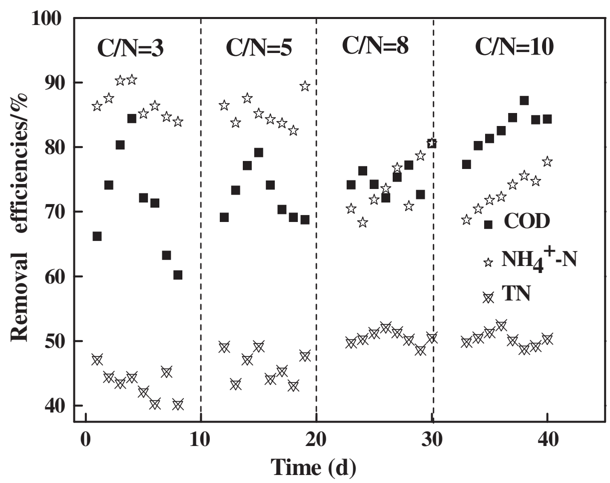

Fig. 7. COD/NH_4^+-N/TN removal performances of the systems at COD/NH_4^+-N ratios of 3–10.

This finding strengthened the assessability of the AACPs and the effect of biofiltration [27–29].

3.4.2. *Effect of COD_{Cr}/NH_4^+-N on NH_4^+-N removal efficiencies*

As shown in Fig. 7, At C/N ratios of 3, 5, 8, and 10, the average removal rates of the corresponding NH_4^+-N were determined as 86.83, 85.37, 73.88, and 73.18%, respectively. These results indicated that compared with that at the C/N ratio of 3, nitrification at the C/N ratio of 8 of NH_4^+-N was not completed prior to discharge from the AACP BAFs.

This finding could be explained as follows: As the concentration of organic matter (COD_{Cr}) increased, large amounts of O_2 (as the electron acceptor) were consumed by the increasing heterotrophic micro-organisms, thereby inhibiting growth rate. The potential of NH_4^+-N removal was considerably affected by the number of nitrifies. Thus, the increase in C/N ratios inevitably decreased the NH_4^+-N removal efficiencies in the biofilters, despite previous literature reported that some heterotrophic organisms can also nitrify the inorganic nitrogen compounds at low DO concentrations [27]. Heterotrophic bacteria and autotrophic bacteria competed for the substrates, DO, and habitat of the medium in the AACP BAFs. Higher organic loading induced by an increase in the C/N ratio could favor heterotrophic bacteria over autotrophic bacteria [30].

3.4.3. *Effect of COD_{Cr}/NH_4^+-N on TN removal*

As shown in Fig. 7, the TN removal efficiencies increased in the biofilters along with the increase in C/N ratios. The lower efficiencies of denitrification at C/N ratios of 3 and 5 were caused by the shortage of carbon source (COD_{Cr}) for the biomass in the anoxic layer. Except for the initial low COD_{Cr} concentration (C/N ratios of 3 and 5), the shortage of carbon source was partly attributed to the mass transfer limitation, which was caused by the low permeability of the biofilm and the high COD_{Cr} utilization rate of the heterotrophic population. This phenomenon also occurred because the oxygen consumption of heterotrophic micro-organisms at low C/N ratios was less than that at high C/N ratios. In addition, more oxygen was available for diffusion to the anoxic layer, resulting in the thinning of anoxic layer and inhibition of denitrifying activity. At C/N ratio of 8, the average removal efficiency of TN in the AACP BAFs biofilters was determined as 50.54%. At the C/N of 10, the average removal efficiency of TN in the biofilters was calculated as 50.34%. From above results, to achieve promising removal efficiency at low C/N ratios, carbon source may be added, like described in literatures [31,32].

3.4.4. *Effect of COD/NH_4^+-N on phosphate removal*

The AACP BAFs were operated at different C/N ratios of 3, 5, 8, and 10, whereas the phosphate concentration of the influent remained in the range of 0.5–0.6 mg/L and HRT was 7.09 h. Fig. 8 shows the phosphate removal efficiencies by the AACP BAFs at different C/N ratios.

With extended operation of the experiment, phosphate removal rate remained almost stable (75.80–91.30%). The mechanism of phosphate removal by AACP BAFs involved a combination effect of physical

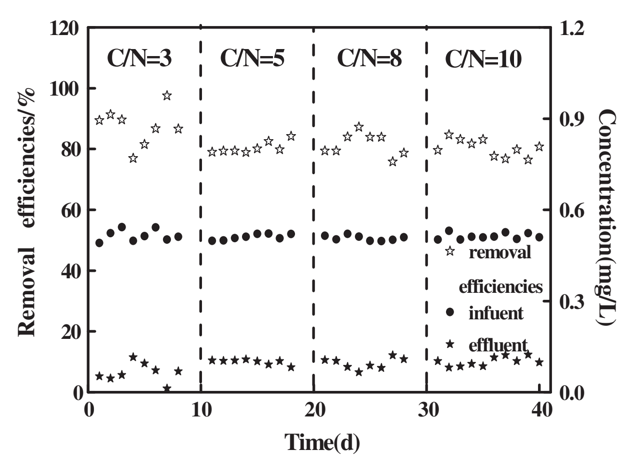

Fig. 8. Phosphate removal performances of the systems at COD/NH_4^+-N ratios of 3–10.

adsorption, chemical reaction, and microbial degradation [33,34]. Metal ions (e.g. Fe^{3+}, Al^{3+}, and Ca^{2+}) can be easily interacted with phosphate. Thus, metal phosphates become adsorbed on the substrate by physical actions and then stored by polyphosphate-accumulating bacteria [35]. This adsorption capacity was small and easily saturated, whereas chemical adsorption by these elements (mainly Al, Fe, and Ca) could continue and thus exhibited long-term stability [36,37].

4. Conclusions

AACPs were tested as biofilter carriers, some conclusions are drawn in the following:

(1) AACPs had a uniform and large-sized internal porosity that can accommodate guest microorganisms.
(2) AACPs can play significant roles as carriers in biological wastewater treatment systems. They had the removal efficiency ranges with 73.12–82.73% for COD, 43.9–51.0% for TN, and 75.8–91.3% for P at a COD_{Cr}/NH_4^+ ratio of 3–10.
(3) The properties of AACPs can significantly affect COD_{Cr}, TN, and phosphate removal efficiencies in the biofilters as they determine the mass transfer of wastewater constituents, permeability of the biofilm, and the extent of contact reactions.

Acknowledgements

We gratefully acknowledge the supports by the National Natural Science Foundation of China (41072036, 41130206, 41202021), the Specialized Research Fund for the Doctoral Program of Higher Education of China (20110111110003).

References

[1] H. Kurama, İ.B. Topçu, C. Karakurt, Properties of the autoclaved aerated concrete produced from coal bottom ash, J. Mater. Process. Technol. 209 (2009) 767–773.
[2] I. Sánchez, X.R. Nóvoa, G. de Vera, M.A. Climent, Microstructural modifications in Portland cement concrete due to forced ionic migration tests, Cem. Concr. Res. 38 (2008) 1015–1025.
[3] H. Kus, K. Nygren, P. Norberg, In-use performance assessment of rendered autoclaved aerated concrete walls by long-term moisture monitoring, Build. Environ. 39 (2004) 677–687.
[4] S. Ghosh, M. Das, S. Chakrabarti, S. Ghatak, Development of ceramic tiles from common clay and blast furnace slag, Ceram. Int. 28 (2002) 393–400.
[5] M. Erol, A. Genç, M.L. Öveçoğlu, E. Yücelen, S. Küçükbayrak, Y. Taptık, Characterization of a glass-ceramic produced from thermal power plant fly ashes, J. Eur. Ceram. Soc. 20 (2000) 2209–2214.
[6] V.K. Marghussian, A. Maghsoodipoor, Fabrication of unglazed floor tiles containing Iranian copper slags, Ceram. Int. 25 (1999) 617–622.
[7] S. Han, Q. Yue, M. Yue, B. Gao, Y. Zhao, W. Cheng, Effect of sludge-fly ash ceramic particles (SFCP) on synthetic wastewater treatment in an A/O combined biological aerated filter, Bioresour. Technol. 100 (2009) 1149–1155.
[8] J. Ha, S. Ong, Nitrification and denitrification in partially aerated biological aerated filter (BAF) with dual size sand media, Water Sci. Technol. 55 (2007) 9–17.
[9] F. Osorio, E. Hontoria, Wastewater treatment with a double-layer submerged biological aerated filter, using waste materials as biofilm support, J. Environ. Manage. 65 (2002) 79–84.
[10] R.E. Moore, J. Quarmby, T. Stephenson, BAF media: Ideal properties and their measurement, Process Saf. Environ. Prot. 77 (1999) 291–297.
[11] C.R. Cheeseman, G.S. Virdi, Properties and microstructure of lightweight aggregate produced from sintered sewage sludge ash, Resour. Conserv. Recycl. 45 (2005) 18–30.
[12] A.P. Picanço, M.V. Vallero, E.P. Gianotti, M. Zaiat, C.E. Blundi, Influence of porosity and composition of supports on the methanogenic biofilm characteristics developed in a fixed bed anaerobic reactor, Water Sci. Technol. 44 (2001) 197–204.
[13] Y. Feng, Y. Yu, L. Qiu, Y. Yang, Z. Li, M. Li, L. Fan, Y. Guo, Impact of sorption functional media (SFM) from zeolite tailings on the removal of ammonia nitrogen in a biological aerated filter, J. Ind. Eng. Chem. 21 (2015) 704–710.
[14] S. Wu, Y. Qi, Q. Yue, B. Gao, Y. Gao, C. Fan, S. He, Preparation of ceramic filler from reusing sewage sludge and application in biological aerated filter for soy protein secondary wastewater treatment, J. Hazard. Mater. 283 (2015) 608–616.
[15] Y. Feng, J. Qi, L. Chi, D. Wang, Z. Wang, K. Li, X. Li, Production of sorption functional media (SFM) from clinoptilolite tailings and its performance investigation in a biological aerated filter (BAF) reactor, J. Hazard. Mater. 246–247 (2013) 61–69.
[16] Y. Liu, F. Du, L. Yuan, H. Zeng, S. Kong, Production of lightweight ceramisite from iron ore tailings and its performance investigation in a biological aerated filter (BAF) reactor, J. Hazard. Mater. 178 (2010) 999–1006.
[17] G.R. Xu, J.L. Zou, G.B. Li, Stabilization of heavy metals in ceramsite made with sewage sludge, J. Hazard. Mater. 152 (2008) 56–61.
[18] L. Qiu, J. Ma, L. Zhang, Characteristics and utilization of biologically aerated filter backwashed sludge, Desalination 208 (2007) 73–80.
[19] J.L. Zou, G.R. Xu, K. Pan, W. Zhou, Y. Dai, X. Wang, D. Zhang, Y. Hu, M. Ma, Nitrogen removal and biofilm structure affected by COD/NH_4^+-N in a biofilter with porous sludge-ceramsite, Sep. Purif. Technol. 94 (2012) 9–15.
[20] Chinese EPA, Methods for Water and Wastewater Analysis, fourth ed., Environmental Science Publishing House of China, Beijing, 2002.

[21] H. Li, Y. Wang, L.Q. Shi, J. Mi, D. Song, X.J. Pan, Distribution and fractions of phosphorus and nitrogen in surface sediments from Dianchi Lake, China, Int. J. Environ. Res. 6 (2011) 195–208.
[22] K. Ruzyla, D.I. Jezek, Staining method for recognition of pore space in thin and polished sections, J. Sediment. Res. 57 (1987) 777–778.
[23] C. Wu, S. Ushiwaka, H. Horii, K. Yamagiwa, Membrane-attached biofilm as a mean to facilitate nitrification in activated sludge process and its effect on the microfaunal population, Biochem. Eng. J. 40 (2008) 430–436.
[24] L.W. Xiao, M. Rodgers, J. Mulqueen, Organic carbon and nitrogen removal from a strong wastewater using a denitrifying suspended growth reactor and a horizontal-flow biofilm reactor, Bioresour. Technol. 98 (2007) 739–744.
[25] E. Ramírez-López, J. Corona-Hernández, L. Dendooven, P. Rangel, F. Thalasso, Characterization of five agricultural by-products as potential biofilter carriers, Bioresour. Technol. 88 (2003) 259–263.
[26] M. Martín-Cereceda, B. Pérez-Uz, S. Serrano, A. Guinea, Dynamics of protozoan and metazoan communities in a full scale wastewater treatment plant by rotating biological contactors, Microbiol. Res. 156 (2001) 225–238.
[27] K. Nootong, W.K. Shieh, Analysis of an upflow bioreactor system for nitrogen removal via autotrophic nitrification and denitrification, Bioresour. Technol. 99 (2008) 6292–6298.
[28] T. Osaka, K. Shirotani, S. Yoshie, S. Tsuneda, Effects of carbon source on denitrification efficiency and microbial community structure in a saline wastewater treatment process, Water Res. 42 (2008) 3709–3718.
[29] A. Patel, J. Zhu, G. Nakhla, Simultaneous carbon, nitrogen and phosphorous removal from municipal wastewater in a circulating fluidized bed bioreactor, Chemosphere 65 (2006) 1103–1112.
[30] C. Zhang, Y. Chen, Simultaneous nitrogen and phosphorus recovery from sludge-fermentation liquid mixture and application of the fermentation liquid to enhance municipal wastewater biological nutrient removal, Environ. Sci. Technol. 43 (2009) 6164–6170.
[31] Y. Chiu, L. Lee, C. Chang, A.C. Chao, Control of carbon and ammonium ratio for simultaneous nitrification and denitrification in a sequencing batch bioreactor, Int. Biodeterior. Biodegrad. 59 (2007) 1–7.
[32] K.A. Third, B. Gibbs, M. Newland, R. Cord-Ruwisch, Long-term aeration management for improved N-removal via SND in a sequencing batch reactor, Water Res. 39 (2005) 3523–3530.
[33] Y.Z. Li, Y.L. He, D.G. Ohandja, J. Ji, J.F. Li, T. Zhou, Simultaneous nitrification–denitrification achieved by an innovative internal-loop airlift MBR: Comparative study, Bioresour. Technol. 99 (2008) 5867–5872.
[34] M. Özacar, Equilibrium and kinetic modelling of adsorption of phosphorus on calcined alunite, Adsorption 9 (2003) 125–132.
[35] W. Zhang, F. Hou, Y. Peng, Q. Liu, S. Wang, Optimizing aeration rate in an external nitrification–denitrifying phosphorus removal (ENDPR) system for domestic wastewater treatment, Chem. Eng. J. 245 (2014) 342–347.
[36] M.E. Kvarnström, C.A. Morel, T. Krogstad, Plant-availability of phosphorus in filter substrates derived from small-scale wastewater treatment systems, Ecol. Eng. 22 (2004) 1–15.
[37] Y. Kong, J.L. Nielsen, P.H. Nielsen, Identity and ecophysiology of uncultured actinobacterial polyphosphate-accumulating organisms in full-scale enhanced biological phosphorus removal plants, Appl. Environ. Microbiol. 71 (2005) 4076–4085.